Crystallization and Spectroscopic Properties of Electron-Beam-Deposited, Chromium-Doped, Forsterite Films

Jennifer L. Mass,[†] James M. Burlitch,*[,†] Duane B. Barber,[‡] and Clifford R. Pollock[‡]

Department of Chemistry and Chemical Biology, Baker Laboratory, and School of Electrical Engineering, Cornell University, Ithaca, New York 14853

Received March 19, 1999

A sol−gel prepared, chromium-doped, magnesium- and silicon-containing oxide mixture was used as a target material for the electron-beam deposition of 1.2 μm thick chromium-doped forsterite films onto single-crystal quartz substrates. The stoichiometry of the target materials was adjusted to compensate for the disparate volatilities of the component oxides. X-ray diffraction revealed that the as-deposited films were amorphous, and the refractive indices of the films revealed that they were near full density. Heating the films to 650 °C produced isolated crystallites of forsterite that ranged in size from 50 to 250 nm in an amorphous matrix (by TEM). Only films that had been heated to 725 °C and above revealed Cr^{4+} emissions.

Introduction

Chromium-doped forsterite ($Cr:Mg_2SiO_4$) is a tunable solid-state lasing material in the near-infrared.[1−6] Its near-IR emission extends from 1.17 to 1.35 μm and encompasses 1.31 μm, the wavelength of light used to transmit information through much of the world's fiber-optic communications networks. This makes $Cr:Mg_2SiO_4$ an appealing material for application as an optical waveguide amplifier in fiber-optic networks. Optical waveguide amplifiers can potentially lower the cost of information transport since they will allow for longer distances between regenerators (extension of transmission distances) and can be used to allow for less sensitive receivers.[7]

Neodymium(III)-doped silica fibers were initially explored for use at 1.31 μm, but the Nd^{3+} transition at 1300 nm suffers from excited-state absorption which prohibits gain at wavelengths shorter than 1360 nm.[8] Praseodymium(III)-doped fluoride glasses such as Pr:ZBLAN, (ZBLAN = $ZrF_4BaF_2LaF_3AlF_3NaF$) have also been explored for potential use in this region.[9] Praseodymium has a laser line at 1300 nm, but cannot currently be pumped with a diode laser (Ti:sapphire lasers are used for this purpose) and so has not found commercial application.[9] Since forsterite cannot be drawn into fibers and Cr^{4+} does not have an emission in forsterite glass, chromium-doped forsterite optical waveguide amplifiers with thin film morphologies are desirable.[10,11] This paper will discuss the deposition of thin films of chromium-doped forsterite by the electron-beam method using sol−gel-derived target materials. Since the films are intended for use as waveguides, in this study they were deposited only onto materials with refractive indices lower than forsterite (1.66 average RI).[12]

Electron-beam deposition was selected as the best route to a 1.2 μm thick $Cr:Mg_2SiO_4$ film since direct spin-coating of a $Cr:Mg_2SiO_4$ sol could not be used to prepare films greater than 0.9 μm thick (due to cracking problems).[13] The sol−gel method was applied to the preparation of polycrystalline powders for use as electron-beam deposition targets.

Since different materials will have different evaporation coefficients and vapor pressures in the electron-beam deposition of alloys and compounds, the vapor plume will have a different composition than that of the target material. The components with higher vapor pressures will be vaporized more rapidly, become enriched in the vapor plume, and subsequently be enriched in the deposited film.[14,15]

* To whom correspondence should be addressed.
[†] Department of Chemistry and Chemical Biology.
[‡] School of Electrical Engineering.

(1) Petricevic, V.; Gayen, S. K.; Alfano, R. R.; Yamagishi, K.; Anzai, H.; Yamaguchi, Y. *Appl.Phys. Lett.* **1988**, *52*, 1040−1042.
(2) Petricevic, V.; Gayen, S. K.; Alfano, R. R. *Appl. Phys. Lett.* **1988**, *53*, 2590−2592.
(3) Agnesi, A.; Piccinini, E.; and Reali, G. C. *Opt. Commun.* **1997**, *135*, 77−82.
(4) Fijii, T.; Nagano, M.; Kemoto, K. *IEEE J. Quantum Electron.* **1996**, *32*(8) 1497−1503.
(5) Agnesi, A.; Dell Acqua, S.; Gobbi, P. G. *Opt. Commun.* **1996**, *127*, 273−276.
(6) Ahmad, H. B.; McKinnie, I. T. *Opt. Laser Technol.* **1995**, *27*, 403−406.
(7) Carts, Y. A. *Laser Focus World* **1990**, *26* (7), 149.
(8) Morkel, P. R. *Opt. Commun.* **1988**, *67*, 349−352.
(9) Ohishi, Y.; Kanamori, S.; Nishi, T.; Takahashi, S. *IEEE Photon. Technol. Lett.*, **1991**, *3*, 715.
(10) Hommerich, U.; Eilers, H.; Yen, W. M.; Hayden, J. S.; Aston, M. K. *J. Luminesc.* **1994**, *60&61*, 119−122.
(11) Beecroft, L. L.; Ober, C. K. *Chem. Mater.* **1997**, *9*, 1302−1317.
(12) Deer, W. A.; Howie, R. A.; Zussman, J. *An Introduction to the Rock-Forming Minerals*; Longman Scientific and Technical: Harlow, England, 1992; p 3.
(13) Park, D. G., Ph.D. Dissertation, Cornell University, 1994.
(14) *Energy-Beam Processing of Materials: Advanced Manufacturing Using Various Energy Sources*; Taniguchi, N., Ikeda, M., Miyamoto, I., Miyazaki, T., Ed.; Clarendon Press: Oxford, England, **1989**, 182−187.

10.1021/cm990162y CCC: $18.00
Published on Web 07/16/1999

Although electron beam deposition has been frequently used in the preparation of multicomponent oxide ceramic coatings, the change in composition from the target material to deposited film remains a continuing problem.[15−18] To attempt to reproduce the exact stoichiometry of the target material in the growing film, several modifications of traditional electron beam evaporation have been developed. Flash evaporation, a technique that involves premelting and quantitative deposition of the target, has been explored for the preparation of superconducting oxide materials such as YBaCuO and BiCaSrCuO films.[17,19] The multiple source evaporation method, involving the use of automated rotating crucibles, has been used for the preparation of cerium dioxide and silicon dioxide thin film composites.[15]

These methods are not without problems, however, and this makes the development of a new method desirable. Multisource evaporation techniques suffer from serious problems in the control of the compositions of the deposited films and also require large amounts of hearth space in the deposition chamber that may not be available.[15] Flash evaporation offers an improvement in the stoichiometry of the prepared films with respect to the target materials but does not solve the stoichiometry problem completely.[15] These considerations led to the development of a sol−gel method of target material preparation that enables one to correct for the disparate volatilities of the component oxides before the deposition.

Experimental Section

General Comments. Polished z-cut single-crystal quartz substrates were obtained from Meller Optics Inc. Polished ⟨100⟩ silicon wafer substrates were purchased from Unisil. Substrates were cleaned with an Applied Surface Technologies Inc. CO_2 Snowjet gun prior to depositions. A Scintag PAD X diffractometer was used to collect all X-ray diffraction data using copper radiation. Optical micrographs were obtained using a Leitz Laborlux 12 HL microscope. Electron-beam depositions were performed in the Technical Operations Laboratory at the Cornell Center for Materials Research (CCMR). Rutherford backscattering spectroscopy (RBS) of the as-deposited films was performed at the CCMR ion facility. Modeling of the spectra was performed with a modified version of the RUMP code for conventional RBS spectral analysis.[19−21] The error in spectral modeling from this method is ±5%. Ellipsometry was performed on a Rudolph Auto-El ellipsometer; the wavelength of light used for refractive index determination was 632.8 nm. Emission spectra were obtained using a pump laser at 1064 nm (Nd:YAG) or at 514.5 nm (argon ion) to excite the $Cr:Mg_2SiO_4$ film. A scanning monochromator, with either a silicon or germanium detector, was used to record the resulting spectra. Transmission electron microscopy was performed on a JEOL 1200EX microscope.

Target Material Preparation. A chromium-doped (8×10^{-5} mol) methanolic solution of magnesium (0.298 mol) and silicon (0.118 mol) methoxides (Mg/Si molar ratio of 2.53 and Cr/Si molar ratio of 6.58×10^{-4}) was prepared using chromium trioxide as a chromium source according to the technique previously used for the synthesis of $Cr,Al:Mg_2SiO_4$.[22] The sol was hydrolyzed using the hydrogen peroxide-assisted method that has been developed for the sol−gel synthesis of forsterite and olivine.[23,24,13] This method involves the slow addition (via a syringe pump) of a dilute methanolic solution of 30% hydrogen peroxide (sufficient to hydrolyze 75% of the OR groups) to the reaction mixture. The solvent was evaporated from the resulting clear bright yellow sol, and the remaining xerogel was ground into a powder and fired in air using fused silica crucibles. The powder was heated to 300 °C at a rate of 1.5°/min, calcined at 300 °C for seven h, heated to 1000 °C at a rate of 1.67 °C/min, and fired at 1000 °C for 7 h. The resulting pink fired powder was pressed into 13 mm diameter × 2−3 mm thick pellets, and sintered at 1100 °C for 12 h.

Electron-Beam Deposition. Two silicon wafer substrates (1 cm × 1 cm) and two low refractive index substrates (either fused silica or z-cut single-crystal quartz) were cleaned using high-pressure blasts of carbon dioxide (CO_2 from an Applied Surface Technologies Inc. Snowjet gun), and they were mounted to the top of the vacuum chamber using conductive silver paint.[25] The sintered targets were loaded directly onto the water-cooled copper hearth without the use of a crucible. The chamber was then evacuated to a pressure of 1.8×10^{-7} mmHg, and oxygen gas was bled into the system up to a pressure of 5×10^{-5} mmHg during the deposition. The progress of the deposition was monitored by a quartz oscillator, which was calibrated using Rutherford backscattering thickness data. Deposition rates of 10−15 or 30−40 Å/s were used.

Characterization. Using a diamond-edged wafering blade, each fused silica or single-crystal quartz substrate was cut into quarters for analysis. The films on low index substrates were examined by X-ray diffraction, TEM, optical microscopy, and optical spectroscopy, and the films on Si(100) were examined by ellipsometry and RBS. To obtain X-ray patterns from the films, a scan speed of 1.5°/min was required. Samples for TEM analysis were prepared by either pressing flakes of the film onto a copper grid coated with TEM grid glue (an adhesive dissolved in ethylene dichloride) or by trapping flakes of the film between folding "oyster" grids that were coated on one side with Fomvar films. All samples for TEM analysis were coated with 250 Å of a conducting carbon film.

Crystallization. Crystallization experiments were only performed on the fused silica and single-crystal quartz substrate films. The films were placed in Al_2O_3 boats, and they were heated in air in a box furnace at a rate of 30 °C/h to temperatures of between 600 and 1100 °C. Crystallized films were analyzed by optical microscopy, X-ray diffraction, TEM, and emission spectroscopy. One of the films used to study the emission spectra as a function of temperature (see Figure 3c) was heated under flowing oxygen at ramp rates of 30 °C/h in a tube furnace.

Results and Discussion

Target Material Preparation. To achieve the desired stoichiometry of $0.005\ Cr:Mg_2SiO_4$ in the deposited film, the target material sols were prepared with a stoichoimetry of $xCr:Mg_2Si_{0.79}O_4$ where $x = 0.00052-0.0008$. This stoichiometry corrected for the volatility differences of the component metal oxides (SiO_2 bp, 2230

(15) Shivalingappa, L.; Narasimha Rao, K.; Mohan, S. *Vacuum* **1993**, *44*, 1031−1035.
(16) Davis, M. F.; Wosik, J. L.; Wolfe, J. C. *J. Appl. Phys.* **1989**, *66*, 4903−4908.
(17) Mogro-Campero, A.; Hunt, B. D.; Turner, L. G.; Burrell, M. C.; Balz, W. E. *Appl. Phys. Lett.* **1988**, *52*, 584−586.
(18) Osofsky, M. S.; Lubitz, P.; Harford, M. Z.; Singh, A. K.; Qadri, S. B.; Skelton, E. F.; Elam, W. T.; Soulen, R. J.; Lechter, W. L.; Wolf, S. A. *Appl. Phys. Lett.* **1988**, *53*, 1663−1664.
(19) Doolittle, L. R. *Nucl. Instrum. Methods Phys. Res.* **1985**, *B9*, 344.
(20) Li, J.; Vizkelethy, G.; Revesz, P.; Mayer, J.; Matienzo, L.; Emmi, F.; Ortega, C.; Siejka, J. *Appl. Phys. Lett.* **1990**, *58*, 1334.
(21) Vizkelethy, G.; Revesz, P.; Mayer, J.; Li, J. *SIA* **1993**, *20*, 309−316.
(22) Mass, J. L.; Burlitch, J. M.; Budil, D. E.; Freed, J. H.; Barber, D. B.; Pollock, C. R.; Higuchi, M.; Dieckmann, R. *Chem. Mater.* **1995**, *7*, 1008−1014.
(23) Park, D. G.; Burlitch, J. M.; Geray, R. F.; Dieckmann, R.; Barber, D. B.; Pollock, C. R. *Chem. Mater.* **1993**, *5*, 518.
(24) Burlitch, J. M.; Beeman, M. L.; Riley, B.; Kohlstedt, D. L. *Chem. Mater.* **1991**, *3*, 692−698, and references therein.
(25) Sherman, R.; Hirt, D.; Vane, R. *J. Vacuum Sci. Technol.* **1994**, *12*, 1876−1881.

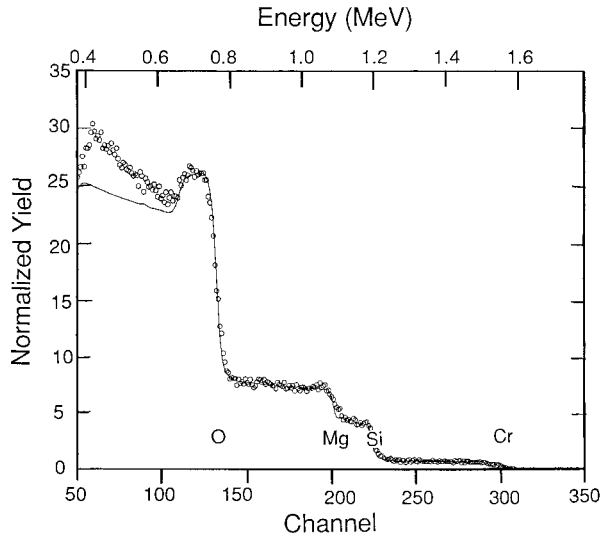

Figure 1. He^{2+} (2.14 MeV) RBS spectrum of a 1.35 μm film deposited from a Cr:Mg_2SiO_4 target (Cr/Si atomic ratio of 0.005).

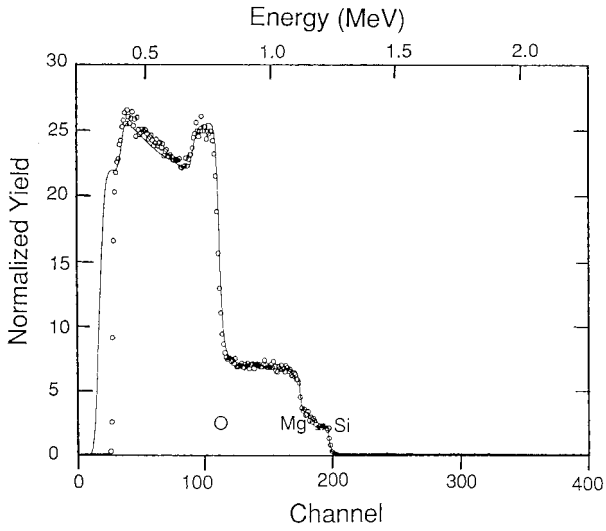

Figure 2. He^{2+} (2.17 MeV) RBS spectrum of a 0.65 μm film deposited from a Cr:$Mg_2Si_{0.79}O_4$ target (Cr/Si atomic ratio of 0.001).

Table 1. Rutherford Backscattering Compositional Data for Electron-Beam Target Materials and Films

sample	initial composition	composition after deposition
1	0.01 Cr:Mg_2SiO_4	0.10 Cr:$Mg_2Si_{1.27}O_{4.1}$
2	0.0008 Cr:$Mg_2Si_{0.79}O_4$	0.005 Cr:$Mg_2Si_{0.9}O_4$

°C; MgO bp, 3600 °C; CrO_3 mp, 196 °C). The necessary target stoichiometry was determined by conducting preliminary experiments using 0.01 Cr:Mg_2SiO_4 pressed pellet targets. The degree of chromium and silicon enrichment in the films resulting from these experiments, measured by RBS, was used to calculate the extent to which subsequent target materials should be depleted in chromium and silicon to produce the desired stoichiometry (see Table 1).

X-ray diffraction analysis of the 0.0005 Cr:$Mg_2Si_{0.79}O_4$ target material powder revealed it to be a mixture of forsterite and periclase (MgO). The presence of periclase is due to the excess of magnesium in the material relative to the composition of forsterite. Since the ratios of CrO_3, $Si(OEt)_4$, and Mg^0 starting materials could be easily altered, the sol−gel method proved to be ideal for the preparation of target materials with precisely controlled stoichoimetries.

Deposition Conditions. Fused silica (RI = 1.45), single-crystal quartz (RI = 1.54), and silicon wafer substrates were employed for the electron-beam depositions. During the depositions, oxygen gas was bled into the vacuum chamber in order to prevent depletion of oxygen in the thin films. This depletion is known to occur during the electron-beam deposition of many oxides.[17] The target material for each deposition was placed directly on the copper hearth, since the use of either tungsten or graphite boats led to contamination of the films (observable by RBS). All films were deposited to a nominal thickness of 1.2 μm (using the quartz oscillator microbalance) unless otherwise stated. Initially deposition rates of 30−40 Å/s were used, but this deposition rate led to sputtering of the target material onto the films. In addition, the films deposited at 30−40 Å/s would shatter more readily upon heating, possibly indicating the presence of trapped porosity. Films prepared at 10−14 Å/s showed fewer overall defects and were less subject to contamination by sputtering of the target.

Characterization. Rutherford backscattering spectrometry was used to examine the stoichiometries of the as-deposited films. The RBS spectrum of a thin film that was prepared using 0.01 Cr:Mg_2SiO_4 pellets as target material revealed a stoichiometry of 0.1 Cr:$Mg_2Si_{1.27}O_{4.1}$ (see Figure 1). The film is enriched in silicon and chromium relative to the target material composition due to the higher volatilities of the silicon and chromium oxides relative to that of periclase. Subsequent targets were prepared with stoichiometries that were altered to reflect the volatility differences of the component oxides (see Table 1). RBS analysis of a film prepared from the stoichiometrically corrected target material revealed an improved composition of 0.005 Cr:$Mg_2Si_{0.9}O_4$ (see Figure 2).

The refractive index of the as-deposited amorphous film was 1.66 (by ellipsometry at 632.8 nm), indicating that the film was near full density upon deposition (forsterite has an aveverage RI of 1.66 at 632.8 nm).[12] If the film had contained significant porosity, it would be revealed as a decrease in the refractive index from that of the bulk material Although in some systems (viz., SiO_2) the refractive index of the amorphous material is lower than that of the crystalline material due to a greater volume of free space, this is not the case with forsterite.[26] Raman spectroscopic and electron diffraction studies have shown that the SiO_4^{4-} tetrahedra in amorphous forsterite have shorter Si−O bond lengths than those in crystalline forsterite.[27] The density of amorphous forsterite, therefore, has the potential to be equivalent to or even slightly greater than that of crystalline forsterite, but the exact value will depend on the amount of free space in the particular sample.[27] The refractive index of the electron-beam deposited forsterite, 1.66 at 632.8 nm, indicates that amorphous forsterite prepared in this manner has nearly the same

(26) Washburn, E. W. *International Critical Tables of Numerical Data; Physics, Chemistry, and Technology;* McGraw-Hill: New York, 1986; Vol. 6, p 341.

(27) Cooney, T. F.; Sharma, S. K. *J. Non-Cryst. Solids* **1990**, *122*, 10−32.

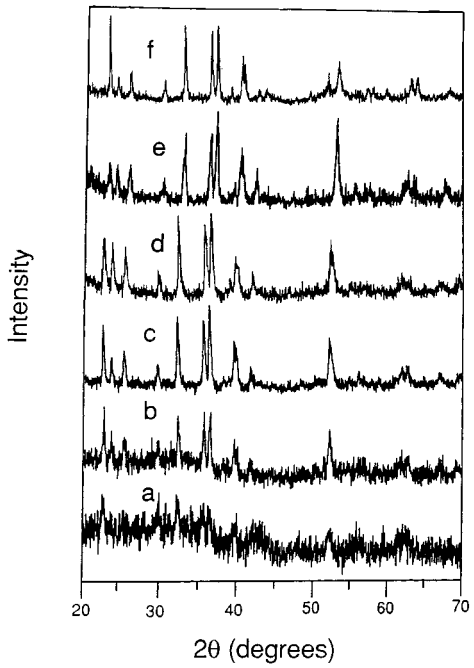

Figure 3. X-ray diffraction patterns of 1.2 μm chromium-doped forsterite films after heating: (a) at 650 °C for 2 h; (b) at 675 °C for 2 h; (c) at 700 °C for 2 h; (d) at 800 °C for 2 h; (e) at 900 °C for 12 h; (f) at 900 °C for 24 h.

density as crystalline forsterite. The refractive indices of the films did not change upon crystallization.

X-ray diffraction of the as-deposited films revealed them to be amorphous. The glassy nature of the films is most likely a result of the limited diffusion possible at the substrate since the depositions were performed at room temperature. The amorphous films did not display any near-IR emission when pumped by either an Ar-ion laser or a Nd:YAG laser. Although Cr^{4+} emission has been previously observed in chromium-doped silicate glasses, it is not observed in glass with the forsterite composition.[10] These findings support the hypothesis that a specific geometrical configuration of the oxygen ligands in the psuedotetrahedral site of the silicate structure is necessary to observe the Cr^{4+} emission.[28,29] X-ray diffraction revealed that amorphous films were obtained even when a deposition was performed with the subtrates at 400 °C, the highest possible substrate temperature that was available experimentally.

Optical microscopy of the films before heat treatment revealed the presence of occasional bubbles and pinholes on the surface of the films but no cracking or island formation. The presence of the bubbles may have been due to contaminants on the surface of the substrates. This type of defect was minimized with the use of carbon dioxide cleaning of the substrates before deposition, but could not be eliminated entirely.[25] The source of pinholes was most likely sputtering of the insulating target material throughout the chamber during the depositions. To minimize pinhole formation, after initial experiments, the deposition rate was decreased from 30−40 to 10−15 Å/s. During the course of the slower depositions, no sputtering was observed, and optical microscopy showed a substantial decrease in pinhole formation.

Crystallization. To be useful as a waveguide, light must be able to propagate uninterrupted down the length of a forsterite film with minimal loss due to scattering. In addition, to be useful as an optical amplifier, a portion of the film has to be crystalline so that the entering near-infrared signal will be increased as a result of stimulating emission from excited laser centers in the waveguide. To meet both of these requirements, the desired system for an optical waveguide amplifier was determined to be isolated 100 nm forsterite crystallites in a glassy forsterite matrix (see below).

To eliminate light scattering at the interface of the matrix and crystallites, the RI of the crystallites should be equal to the RI of the matrix. Since forsterite is a biaxial system, a perfect match of the refractive index of the matrix with the refractive index of the crystallites for all crystallite orientations will not be possible. The α, β, and γ refractive indices for forsterite are 1.635, 1.651, and 1.670 respectively,[12] whereas the refractive index of the amorphous forsterite is 1.66.

According to Rayleigh scattering theory, the scattering losses of the composite will decrease with the square of the index mismatch and with the first power of the scatterer volume.[30] Since the refractive indices of the materials in the composite cannot be altered in an easily controlled manner, the logical way to decrease scattering losses is to decrease the crystallite size. Rayleigh scattering theory predicts a size of 158 nm or smaller in order to have 4% per cm scattering losses for an interaction with 1.2 μm light. To obtain such a scattering loss, the parameters used are an index mismatch of 0.025 (1.66−1.635), a scatterer density (ρ) of 1 scatterer/μm, and a λ of 1.2 μm. Since Rayleigh scattering theory does not take into account other factors such as losses due to defects in the host material, a conservative maximum scatterer diameter of 100 nm was selected as a goal. As a result of these considerations, a firing program was designed for the forsterite glass films that would result in the formation of isolated crystallites ≤100 nm and not in fully crystallized films.

An additional issue related to scattering losses that should be considered is how the dispersion curves of crystalline and amorphous forsterite differ. If the wavelength dependence of the amorphous and crystalline materials' refractive indices differ substantially, then closely matching values at 632.8 nm will not be a good indication of potential scattering losses when the material is used at 1.2 μm. Since the dispersion curve of amorphous forsterite is not known, this problem remains as a potential source of error.

Attempts to crystallize any of the 1.2 μm thick amorphous forsterite films deposited on fused silica substrates without cracking or formation of islands were unsuccessful. An attempt was made to crystallize a thinner 0.3 μm Cr:Mg_2SiO_4 film on a fused silica substrate, but at 800 °C, optical microscopy revealed that the sample had broken apart into square islands of approximately 700 nm. Optical microscopy of the samples heated to 1000 °C and above always revealed

(28) Budil, D. E.; Park, D. G.; Burlitch, J. M.; Geray, R. F.; Dieckmann, R.; Freed, J. H. *J. Chem. Phys.* **1994**, *101*, 3538−3548.
(29) Whitmore, M. H.; Sacra, A.; Singel, D. J. *J. Chem. Phys.* **1993**, *98*, 3656−3664.
(30) Wood, R. W. *Physical Optics*; Macmillan Publishing Co.: New York, 1936.

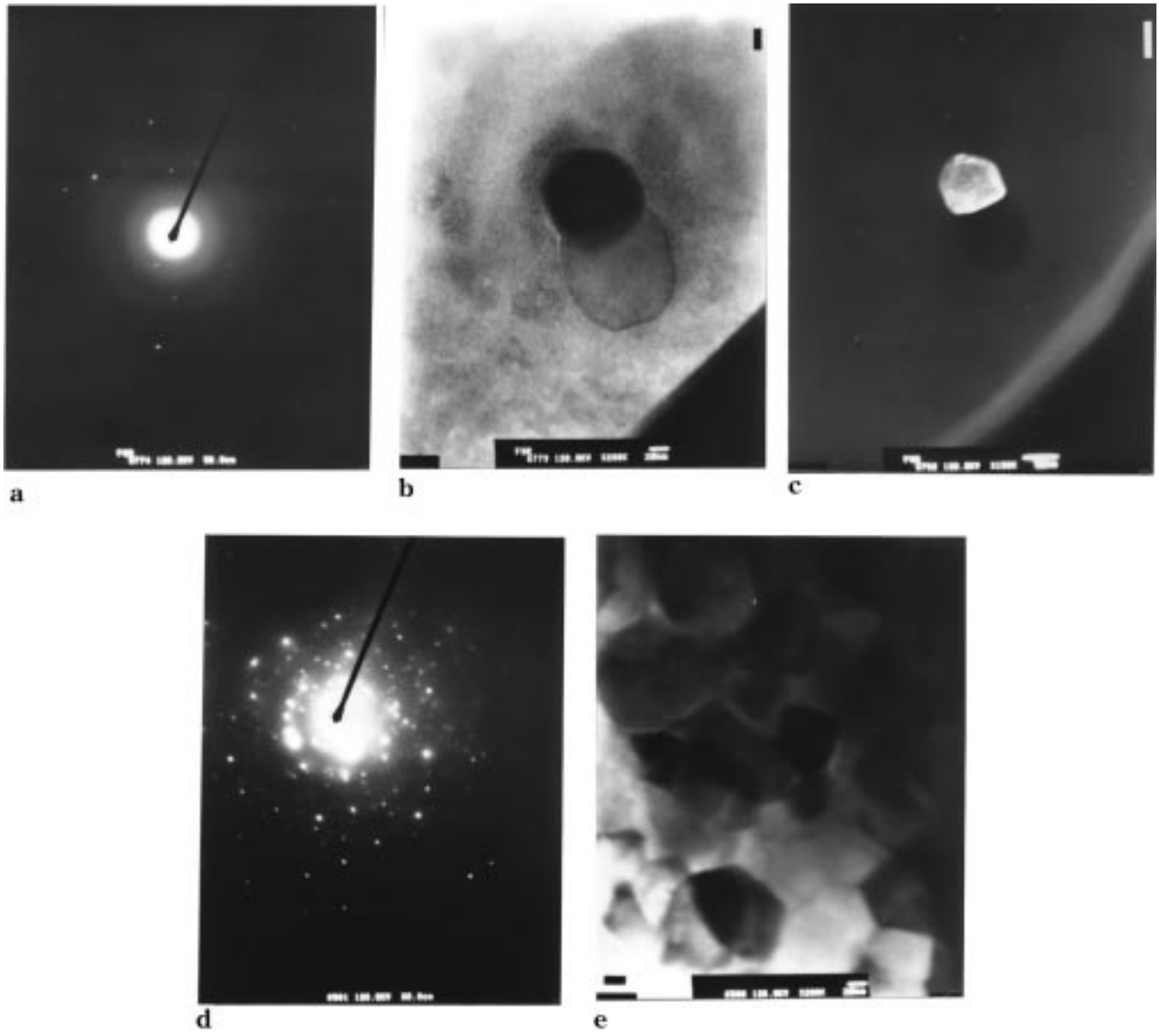

Figure 4. TEM photomicrographs of electron-beam-deposited forsterite films crystallized at 650 and 675 °C: (a) diffraction pattern of film heated to 650 °C; (b) bright field image of film heated to 650 °C (bar = 20 nm); (c) dark field image of film heated to 650 °C (bar = 50 nm); (d) diffraction pattern of film heated to 675 °C; (e) bright field image of film heated to 675 °C (bar = 20 nm).

a characteristic "mudflat" pattern of 1 μm cracks and approximately 10 μm domains. These effects occurred regardless of the heating rates tried (between 0.5 °C/min and 1.67 °C/min), and were observed at temperatures as low as 600 °C. The cracking problem precluded the further use of fused silica substrates in this study, since it took place below the onset of crystallization of forsterite in the films, which occurred at ~650 °C.

The cracking of the films on the fused silica substrates is attributed to the difference in the coefficients of thermal expansion of forsterite and fused silica (9.5×10^{-6} and 0.55×10^{-6} K^{-1}, respectively).[31] Single-crystal quartz substrates were used for subsequent experiments, based upon the material's higher thermal expansion coefficient (13.4×10^{-6} K^{-1} perpendicular to the *c* axis) and its refractive index, which is lower than that of forsterite and therefore suitable for waveguiding purposes.[31] Even with the use of the single-crystal quartz substrates, heating rates of 30 °C/h were necessary to crystallize the amorphous films without any cracking. One shortcoming of single-crystal quartz substrates is the transition from the α-phase to the β-phase that occurs at 573 °C.[32] In two instances out of approximately 20 crystallization experiments, this phase transition caused the substrate to break when the samples were heated.

Great care had to be taken to make sure that all substrates were free of organic or particulate impurities in order to avoid the formation of small bubbles in the films which would cause flaking upon heating. Cleaning the surfaces of the substrates with carbon dioxide

(31) Touloukian, Y. S., Ed. *Thermophysical Properties of Matter: Thermal Expansion of Non-Metallic Solids*; Plenum Publishing Co.: New York, 1977; Vol. 13.

(32) Laudise, R. A. *The Growth of Single Crystals*; Prentice Hall Inc.: Englewood Cliffs, NJ, 1970; p 18.

minimized these problems. With higher heating rates the cracking and flaking of the films is most likely a result of the slight mismatch between the coefficients of thermal expansion of the film and the substate.

X-ray diffraction patterns of the films that were heated to 650 °C and above displayed the powder pattern for crystalline forsterite (see Figure 3), and no additional peaks were observed.[33] As expected, the peaks grow in sharpness and intensity with temperature, indicating an increase in crystallite size at the higher temperatures. The patterns of the films heated to 650 and 675 °C have high backgrounds at low values of 2θ, which indicates that portions of the films were still amorphous. The films prepared using stoichiometric forsterite as a target material had compositions sufficiently far from that of the mineral that they did not readily or cleanly crystallize upon heating.

Transmission electron microscopy of the films heated to 650 and 675 °C revealed the crystalline and amorphous regions of each film (see Figure 4). Figure 4a, the diffraction pattern of the former film, shows a combination of spots and rings, and indicates that the film contains both crystalline and amorphous regions. The use of "grid glue" in place of Formvar films to mount the samples allowed for the observation of an amorphous background without interference from the polymer film. Bright field images (see Figure 4b) reveal portions of the film that appear to deflect the electron beam to varying degrees. To determine if these areas are forsterite crystallites, dark field imaging was performed using the two beam condition (see Figure 4c).[34] Since one crystallite will act as a single diffracting center for the electron beam, individual crystallites will be highlighted by this method. It can be observed in Figure 4c that the regions of the film that previously appeared as spots in the bright field image are single forsterite crystallites. The crystallites observed by this method in the 650 °C film ranged in size from 50 to 250 nm.

Electron diffraction patterns of one region of the film heated at 675 °C (Figure 4d) revealed only crystalline spots indicating that in this area the film is polycrystalline rather than amorphous with embedded crystallites, as was observed for the 650 °C film. Other areas of the 675 °C film (not shown) were still amorphous, which is in agreement with the amorphous background that was observed in the X-ray pattern. Bright field images of the polycrystalline portion of the film revealed a continuous field of crystallites, ranging in size from 50 to 80 nm in some regions (Figure 4e) and from 20 to 30 nm in others (not shown).

Optical Properties. The optical behavior of the films as a function of firing temperature was investigated in order to determine the minimum temperature (and therefore degree of crystallinity) necessary to obtain a strong Cr^{4+} emission. The film (1.2 μm thick), deposited at 10−14 Å/s) was cut into quarters so that samples prepared under identical conditions could be fired to different temperatures. In the first experiment one sample was heated to 650 °C for 6 h. Excitation using an Ar-ion pump beam revealed very weak emissions centered at 1000 nm, which are attributed to Cr^{3+}. No emissions near 1200 nm (Cr^{4+}) were observed (see Figure 5). Therefore, although TEM data reveal that isolated forsterite crystallites had started to form in the films at 650 °C, there was apparently not a sufficient quantity of crystalline forsterite for the observation of a Cr^{4+} emission. A second possibility is that the crystallites were too small for a near-IR emission to be observed (perhaps due to the high surface-to-volume ratio enhancing nonradiative decay caused by surface defects), since both the crystallites' number and size would be expected to increase with increasing temperature.

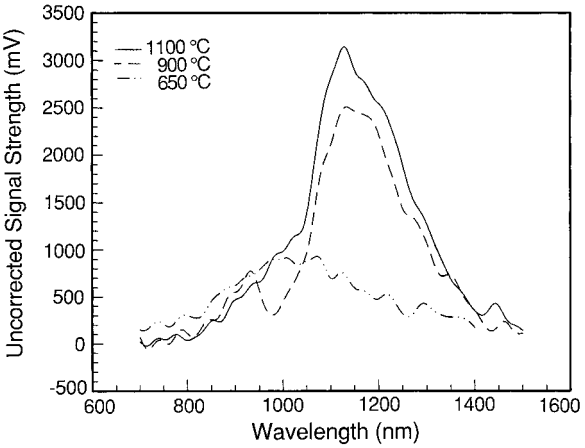

Figure 5. Argon-pumped fluorescence spectra of electron-beam deposited chromium-doped forsterite thin film deposited at 10−14 Å/s, and heated to 650, 900, or 1100 °C.

The next sample, crystallized at 900 °C for 12 h, displayed strong emissions at 1050−1300 nm (Cr^{4+}), and much weaker emissions at 950 nm (Cr^{3+}) when excited with a 2.5 W argon-ion pump beam (see Figure 5). Heating to 1100 °C for 12 h produced even stronger Cr^{4+} emissions than the samples heated to 900 °C (see Figure 5). The films heated to 900 and 1100 °C were processed far above the temperature (675 °C) where TEM studies revealed that polycrystalline regions began to appear in the films (see Figure 4e). Since the grain boundaries in polycrystalline regions may be responsible for light scattering, it was desirable to locate the lowest temperature at which the Cr^{4+} component would dominate a film's near-infrared emission. Toward this end, a 1.2 μm film (deposited at 10−14 Å/s) was heated to 650 °C for 6 h, 675 °C for 12 h, and 725 °C for 12 h, with the aquisition of argon-pumped emission spectra after each firing program. After the film was heated to 650 °C (see Figure 6), the 2.5 W argon-pumped emission spectrum of the film displays only a Cr^{3+} emission. The ratio of the emissions was unchanged after the film was heated to 675 °C (data not shown), but upon heating to 725 °C, the Cr^{4+} emission begins to dominate (Figure 6). Since no Cr^{4+} emission was evident at 675 °C, the temperature at which polycrystalline regions begin to appear in the films, different firing programs may be required to produce a film using these techniques that will both consist of isolated nanocrystallites and also have a bright emission near 1.3 μm.

(33) Morris, M. C.; McMurdie, H. F.; Evans, E. H.; Paretzkin, B.; Parker, H. S.; Wong-Ng, W.; Gladhill, D. M.; Hubbard, C. R. *U.S. Natl. Bur. Stand. Monogr.* **1984,** *25* (20), 71.

(34) Edington, J. W. *Practical Electron Microscopy in Materials Science*; Van Nostrand Reinhold Company: New York, 1976.

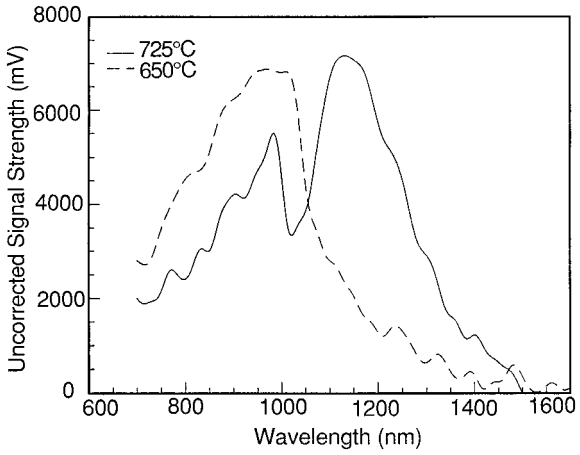

Figure 6. Argon-pumped fluorescence spectra of electron-beam-deposited chromium-doped forsterite thin film deposited at 10−14 Å/s and heated to 650 and 725 °C under flowing oxygen.

Summary and Conclusions

Thin films of chromium-doped forsterite have been deposited by electron-beam methods as glasses on amorphous and crystalline quartz substrates. The films deposited on amorphous silica could not be crystallized at temperatures low enough to avoid film cracking or formation of "islands". The films deposited on crystalline quartz substrates could usually be crystallized intact, but the α to β phase change at 573 °C limits the reliable use of crystalline quartz above this temperature. The films heated to 650 °C had the required degree of crystallinity for waveguiding applications, viz., nanocrystallites embedded in a dense forsterite glass. Only films heated to 725 °C and above, however, displayed chromium-doped forsterite's characteristic Cr^{4+} emission band.

Acknowledgment. The authors thank the Cornell Center for Materials Research (NSF:DMR 91 21654) and the AT&T Foundation for financial support, Gerhard Schmidt for performing the electron-beam depositions, Dr. Peter Revez for collecting the Rutherford backscattering spectra, Enid Karr for help with TEM sample preparation, and Shanthi Submaranian and John Hunt for aquiring the TEM data.

CM990162Y